

Research Article

FeS₂-Quantum-Dot Sensitized Metal Oxide Photoelectrodes: Photoelectrochemistry and Photoinduced Absorption Spectroscopy

Idriss Bedja¹ and Anders Hagfeldt²

¹ CRC, Department of Optometry, College of Applied Medical Sciences, King Saud University, P.O. Box 10219, Riyadh 11433, Saudi Arabia

² Department of Physical Chemistry, Uppsala University, P.O. Box 259, 75105 Uppsala, Sweden

Correspondence should be addressed to Idriss Bedja, bedja@ksu.edu.sa

Received 15 June 2011; Accepted 5 September 2011

Academic Editor: Surya Prakash Singh

Copyright © 2011 I. Bedja and A. Hagfeldt. This is an open access article distributed under the Creative Commons Attribution License, which permits unrestricted use, distribution, and reproduction in any medium, provided the original work is properly cited.

TiO₂, ZnO nanoparticulate(-np), and ZnO-nanorod(-nr) electrodes have been modified with FeS₂ (pyrite) nanoparticles. Quantum size effect is manifested by a blue shift in both absorption and photocurrent action spectra. PIA (photoinduced absorption spectroscopy), a multipurpose tool in the study of dye-sensitized solar cells, is used to study quantum-dot modified metal oxide (MO) nanostructured electrodes. The PIA spectra showed an evidence for long-lived photoinduced charge separation. Time-resolved PIA showed that recombination between electrons and holes occurs on a millisecond timescale. Incident-photon-to-current efficiencies at 400 nm are ranged between 13% and 25%. The better solar cell performance of FeS₂ on ZnO-nr over ZnO-np can be ascribed to the faster, unidirectional e-transport channels through the ZnO-nr as well as the longer electron lifetimes. The lower performances of electrodes can be explained by the presence of FeS₂ phases other than the photoactive pyrite phase, as evidenced from XRD study.

1. Introduction

A great effort is being exerted to obtain efficient and inexpensive organic and inorganic solar cells. The approach of using semiconductor colloids for the design of optically transparent thin semiconductor films is considered as a unique and an alternative for the amorphous silicon solar cells. Under this approach, films made from colloidal metal oxide semiconductors which have large band gap have attained much attention. This is primarily because they are quite stable. In addition, they predominantly absorb in the UV region. The usefulness of these systems for solar cell applications was made possible by a basic principle, namely, sensitization of their semiconductor surfaces into visible region either by organic dyes (dye sensitization) [1–4] or by inorganic short band gap semiconductors also called quantum dots (QDs; semiconductor sensitization) [5–8]. Power conversion efficiencies in the range of 8–12% in diffuse daylight have been

obtained in the ruthenium-based dye-sensitized highly porous TiO₂ film [1]. On the other hand, wide band gap semiconductors have been sensitized by quantum dots, for example, CdSe/TiO₂ [4] and CdS/TiO₂-SnO₂ [8] as alternative to dye sensitization. Vogel and coworkers [6] have investigated the sensitization of nanoporous TiO₂, ZnO, and so forth by Q-sized CdS with the photocurrent quantum yields of up to 80% and open circuit voltages up to 1 V. In contrast with the dye sensitized solar cells, fundamental understanding of factors controlling the interfacial electron transfer reactions for the QD-sensitized solar cells is limited.

Dye sensitized solar cells (DSCs) based on one-dimensional (1D) ZnO nanostructures, which exhibit significantly higher electron mobility than that of both TiO₂ and ZnO-np films [9], have recently been attracting increasing attention [9, 10].

In the present work, instead of organic dye as in DSCs, we used FeS₂ quantum dot semiconductors to sensitize MO

semiconductor thin films ($\text{MO} = \text{TiO}_2$, ZnO-np , and ZnO-nr).

The FeS_2 in pyrite phase is another favorable candidate of photosensitization materials because of its environmental compatibility, and high stability toward photocorrosion as well as its very good absorption in the visible region of the solar spectrum. The pyrite polymorph of iron disulfide is of particular interest, and shows promise for solar energy conversion devices in both photoelectrochemical and photovoltaic solar cells [11, 12] and solid-state solar cells [13] due to its favorable solid state properties [14]. Ennaoui et al. have reported interesting photoresponse of FeS_2 modified polycrystalline TiO_2 electrode [14] using CVD method. Shen et al. [15] have recently reported a method of modification of TiO_2 large band gap (Degussa P25) by quantum-sized FeS_2 particles by a similar procedure described originally by Chatzitheodorou et al. [16]. They reported only an incident-photon-to-current efficiency of 25% at 400 nm excitation and an SEM picture of FeS_2 adsorbed TiO_2 film.

In this work, we report FeS_2 QD sensitized TiO_2 , ZnO-np , and ZnO-nr photoelectrodes prepared by a method described previously by Shen et al. [15]. We described photoelectron-chemical properties and photoinduced absorption spectroscopy for mechanistic study.

2. Experimental

2.1. Preparation of Nanostructured Metal Oxide Film

2.1.1. TiO_2 Nanoparticle Films. FTO plates are first put into a 0.02 M TiCl_4 aqueous solution and kept at 70°C for 30 min. to obtain a thin dense layer of TiO_2 . A paste containing 20 nm sized TiO_2 nanoparticles was subsequently spread on the substrate using a doctor blade method. Working electrodes were then sintered at 450°C for 30 min in a hot air stream.

2.1.2. ZnO Nanoparticle Films. The concentration of ZnO colloids was 0.05 M and was prepared by the method described by Spanhel and Anderson [9] with a little change. Addition of LiOH to the organometallic zinc complex solution was less by 25% than the required for stoichiometric addition. Colloidal ZnO solution thus obtained does not need any further concentration since small amount of solvent was used. The diameter of these colloidal particles was in the range of 2–5 nm. A small aliquot (0.1–0.8 mL) of ZnO sol was applied to the FTO substrate ($0.8 \times 4 \text{ cm}^2$). The films (0.5–3 μm) are dried in air and then heated at 400°C for 1 h. The sintered ZnO films adhered strongly to the FTO surface and were stable in neutral and alkaline solutions.

2.1.3. ZnO -Nanorod Films. Firstly, 300 nm ZnO seed layer was prepared on the FTO-coated glass. Two drops of 5 mM solution of zinc acetate dihydrate in absolute ethanol, rinsed in ethanol and blown dry with nitrogen gas. This is repeated 4 times before sintering at 350°C in air for 30 min. This process is repeated twice. Secondly, the thus ZnO -seeded substrate was immersed into an aqueous solution of 25 mM zinc nitrate hexahydrate, 25 mM hexamethylenetetramine and

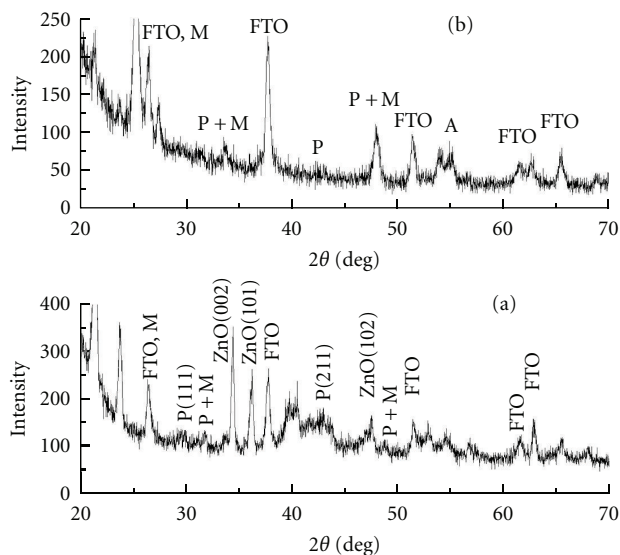


FIGURE 1: XRD spectra of FeS_2 adsorbed metal oxide films. (a) ZnO-nr particulate film and (b) TiO_2 -nanoparticle film. A: anatase; P: pyrite, and M: marcasite.

5 mM polytheleneimine at 90°C for a chemical bath deposition during total 12 hours. The solution was replaced by a fresh one every 4 hours. The obtained ZnO nanorods were rinsed with deionized water and dried in air at room temperature.

2.2. Surface Modification of Metal Oxide Films by FeS_2 Quantum Dots. FeS_2 quantum dots were deposited onto nanostructured metal oxide films using a method to that described by Shen et al. [15], with a little modification. The metal oxide electrode was first dipped in a solution of 0.02 M sulfur in xylene, rinsed with xylene, and heated to 125°C for 5 min, followed by immersion in a solution of 0.01 M iron pentacarbonyl in xylene at a temperature of 139°C , followed by another xylene rinse and heating step (125°C). The whole experiment was carried out in a dry box under a nitrogen atmosphere. This procedure was repeated several times until the electrodes had become significantly darker in appearance.

2.3. Characterization Methods. UV-Vis spectra were recorded using an Ocean Optics HR2000 diode array spectrometer. Photoelectrochemical measurements were carried out using a potentiostat (Princeton Applied Research Model 273) with a 1 cm path-length quartz cuvette as the electrochemical cell. The FeS_2 -modified metal oxide electrode served as a working electrode, a Ag/AgCl (3 M KCl) as reference electrode, and a Pt wire as counter electrode. The electrolyte composition was Na_2S 0.1 M and Na_2SO_4 0.01 M. The setups for recording incident photon to current efficiency (IPCE) spectra and I-V curves have been described elsewhere [17].

For PIA spectroscopy [18], excitation of the sample was provided by a blue LED (Luxeon Star 1 W, Royal Blue, 470 nm), which was square-wave modulated (on/off) by

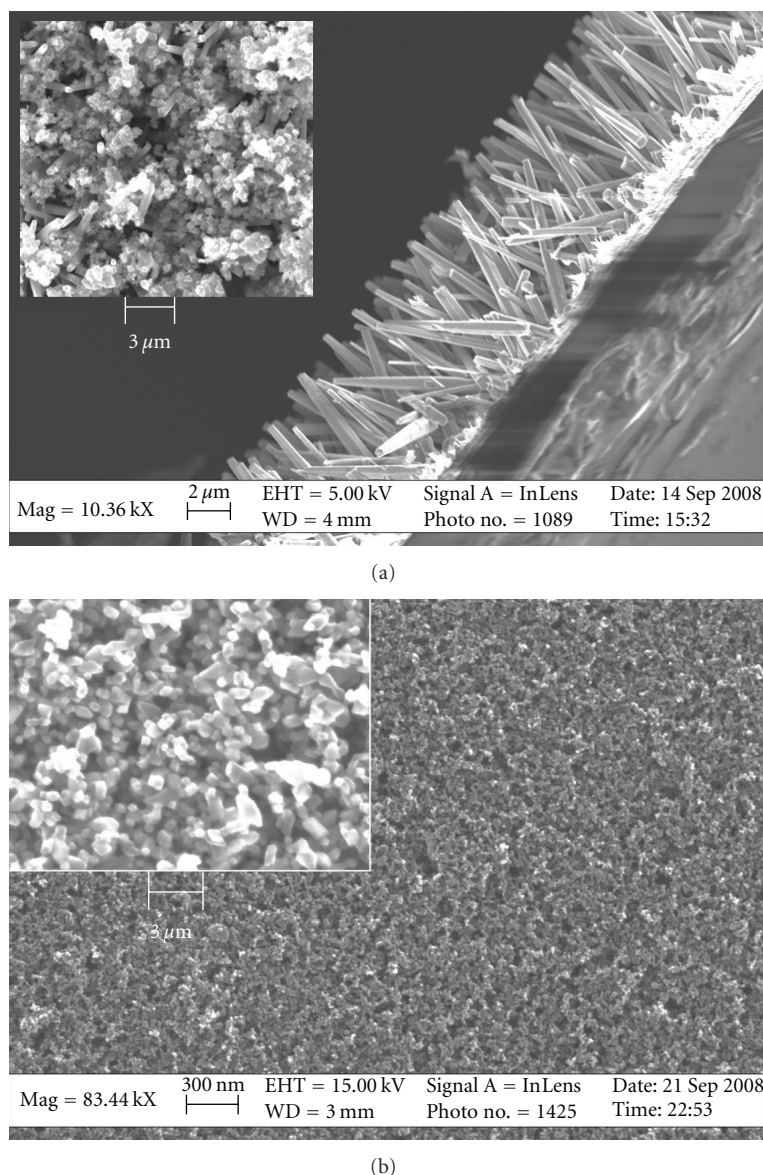


FIGURE 2: Scanning electron microscope images of FeS₂-modified and unmodified metal oxide electrodes. (a) Cross-section of a ZnO nanorod film. Inset: top view of an FeS₂-modified ZnO nanorod film. (b) Top view of TiO₂ nanoparticulate film. Inset: top view of TiO₂ after FeS₂ deposition.

electronical means using an HP 33120A waveform generator and a home-built LED driver system. For the time-resolved studies the output of the current amplifier was connected to a data acquisition board (National Instruments, PCI-6052E). All PIA measurements were done at room temperature.

3. Results and Discussion

3.1. Characterization of FeS₂-Modified Metal Oxide Electrodes. During deposition of FeS₂ onto the metal oxide electrodes, the appearance of the metal oxide electrodes changed from white or transparent to a brown/grey color, which clearly indicates FeS₂ adsorption as confirmed by the XRD study. Figure 1 shows XRD spectra of FeS₂-modified metal oxides. Besides the sharp peaks assigned to SnO₂ (cassiterite) from

the FTO substrate and clear peaks from the metal oxide (ZnO wurtzite, TiO₂ anatase), a number of much smaller and rather poorly resolved peaks also appeared. Possible origin of these peaks are FeS₂ that exists in a cubic phase (pyrite: P) and an orthorhombic phase (marcasite: M). Furthermore hexagonal FeS (troilite) FeO, and so forth may also exist.

The modified metal oxide electrodes were further analyzed using scanning electron microscopy. Figure 2(a) shows a cross section of a ZnO nanorod electrode before modification. The nanorods do not have a parallel orientation as a result of a nonoriented seed layer. The ZnO nanorods that were grown during 12 hours were about 8 μm in length and 300 nm in diameter. The inset clearly shows the deposition of a material in between the ZnO nanorods after the modification procedure. The deposited material, presumable FeS₂,

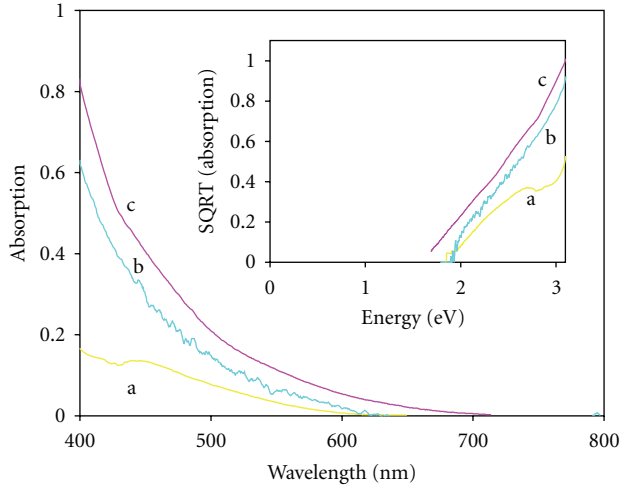


FIGURE 3: Absorption spectra of FeS_2 modified (a) ZnO-np, (b) ZnO-nr, and (c) TiO_2 -np particulate films. Inset: band gap determination from square root of absorbance spectra of FeS_2 -modified metal oxide electrodes: (a) ZnO-np, (b) ZnO-nr, and (c) TiO_2 -np particulate films.

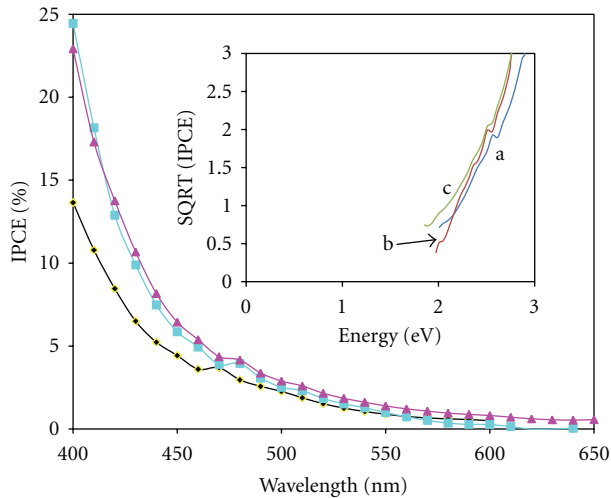


FIGURE 4: IPCE spectra of FeS_2 modified TiO_2 -np (filled triangle), ZnO-nr (filled square), and ZnO-np (filled circle). Inset is a band gap determination from square root of IPCE spectra of FeS_2 -modified metal oxide electrodes: (a) ZnO-np, (b) TiO_2 -np, and (c) ZnO-nr electrodes.

forms rather large aggregated structures. Figure 2(b) shows the top-view of mesoporous TiO_2 films. The inset corresponds to modified TiO_2 films which show formation of large FeS_2 aggregates (sizes between 50–70 nm) on top of TiO_2 nanoparticulate film with less uniformly distributed and dispersed.

UV-Vis absorption spectra (Figure 3) show that the deposited material absorbs light with wavelength lower than 600–700 nm. The low energy tail may come predominately from large particles. However, the high energy absorption shoulders are probably originated from ultrasmall particles. Because FeS_2 has a small band gap around 1 eV [14], we

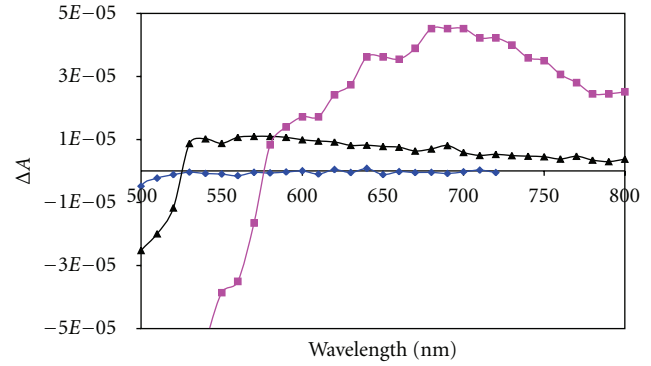


FIGURE 5: Photoinduced absorption spectra of FeS_2 modified metal oxide electrodes in air: TiO_2 -np (filled triangle) ZnO-nr, (filled square), and ZnO-np (filled losange).

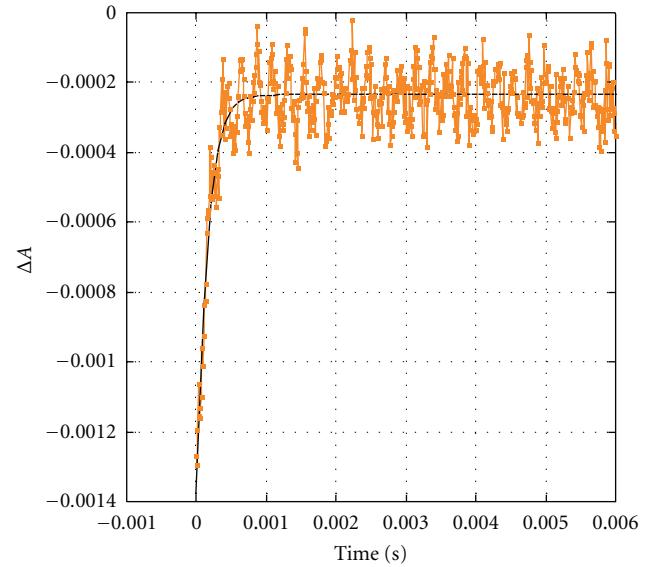


FIGURE 6: PIA decay transient absorption of Q-dots FeS_2 modified ZnO-nanorod electrode after excitation with blue light of 11 mW/cm^2 recorded at 520 nm using a sampling rate of 10^3 s^{-1} and averaged 100 times.

would expect a large wavelength absorption onset near IR. Absorption spectra (Figure 3) show, however, particularly, short wavelength absorption onsets. This might be explained either in term of a quantum size effect of very small FeS_2 particles which causes a band gap energy rising or simply because of nonstoichiometric pyrite present in the film. For this, the band gap of the material was analyzed by plotting (inset of Figure 3) the square root of the absorbance versus photon energy [19]. A linear relation was found for the square root of the absorbance, suggesting that the lowest band gap transition is indirect. The band gap, obtained by extrapolation, may vary between 1.6 and 2.0 eV depending on different metal oxide substrate. The reported value for the band gap of FeS_2 is 0.95 eV [14]. This suggests that there is a strong quantum-size effect due to FeS_2 particles.

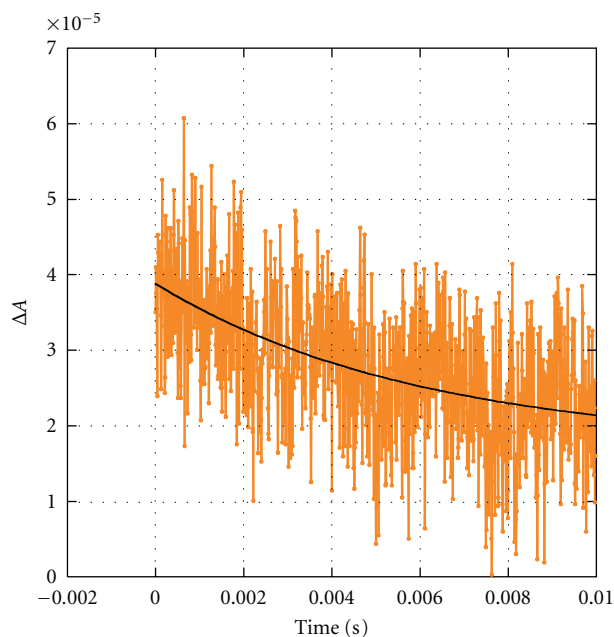


FIGURE 7: PIA decay transient absorption of Q-dots FeS_2 modified TiO_2 electrode after excitation with blue light of 11 mW/cm^2 recorded at 800 nm using a sampling rate of 10^3 s^{-1} and averaged 100 times.

Similarly, IPCE spectra (Figure 4) show essentially the same trend as the absorption spectra. The photoresponse of different metal oxide electrodes have been extended to the visible range after FeS_2 modification. Although the FeS_2/MO electrodes show strong visible absorption in wavelengths longer than 580 nm , no photoresponse was detected at these wavelengths. This suggests that only small quantum-sized FeS_2 particles play a dominant role in the spectral sensitization on TiO_2 particles while larger particles have less or no contribution. In order to validate the indirect band gap of FeS_2 on different MO electrode, the material has been analyzed by plotting the square root of the IPCE versus photon energy (inset of Figure 4). Again, approximately linear relation was found for the square root of the IPCE, suggesting that the lowest band gap transition is indirect. The band gap, obtained by extrapolation, varied approximately between 1.5 and 1.9 eV .

Photoinduced absorption (PIA) spectroscopy, where excitation is provided by an on/off modulated LED or laser giving intensities comparable to one sun is listed here under photoelectrochemical techniques, because it too allows for investigation of dye-sensitized (DSC) or quantum dots-sensitized (SSC) cells under actual operating conditions, and it can easily be combined with simultaneous electrochemical measurements [10, 20]. Small changes in optical transmission are detected using a detector system with a lock in amplifier tuned at the frequency of the modulation. It is very useful in qualitative studies, for instance, to check whether a dye or a quantum dot is injecting electrons into TiO_2 after photoexcitation and whether a dye is regenerated when in contact with a redox electrolyte [21]. The kinetics of slower

processes in the DSC or SSC ($t > 10^{-5} \text{ s}$) can be followed using PIA. Because the PIA signal is proportional to the lifetime of the observed species, it can be sensitive to a small fraction of dye molecules that is not in contact with the redox couple or hole conductor and therefore has a long lifetime of the oxidized state [20].

PIA spectra in Figure 5 shows typical FeS_2 modified different MO electrodes in the absence of the redox electrolyte (in air). The PIA spectra clearly reflect the differential spectrum of FeS_2 upon formation of injected electrons into MO electrode (shown by absorption at large wavelengths), with a bleach of the main absorption of FeS_2 around 470 nm and absorption peak at 580 nm ($\text{TiO}_2\text{-np}$) and 670 nm (ZnO-nr). It has to be noted that no PIA spectrum for pyrite based ZnO-np photoelectrode has been recorded for comparison. This may be due to deep trapped electron sites and large number of boundaries in between ZnO nanoparticles which lead to a very low density of electrons that might leave and decay. For this case, only laser spectroscopy at high pulse intensity could detect that small intensity decay.

The PIA spectra indicate long-live charge separated state occurring in the Q-dot sensitized metal oxides: highest with FeS_2 modified ZnO-nr .

3.2. PIA Kinetics. Study of the kinetics in semiconductor sensitizing solar cells is not only feasible by laser flash photolysis, a costly technique, but also possible using time-resolved PIA measurements. Figure 6 shows an example of such PIA transient; here decay recorded at 520 nm for FeS_2 modified ZnO-nr slow on/off excitation; (pseudo-) first-order rate constant for bleach (growth at 520 nm) was estimated at about 0.15 ms , and is due to hole-electron recombination which also does not follow simple first-order kinetic as for $\text{TiO}_2\text{-np}$ modified with FeS_2 , but is characterized by a range of recombination times. This relatively fast decay also proves at least a well pore filling of ZnO-nr film by ultra fine particles of pyrite.

Similarly, Figure 7 shows PIA transient growth recorded at 800 nm for FeS_2 modified $\text{TiO}_2\text{-np}$. It is clear that the recombination yield between generated electrons and holes does not follow simple first- or even second-order kinetics, but is characterized by a range of recombination times. This has been explained by trapping of electrons within the TiO_2 nanocrystals [20, 22]. Transport of electrons through TiO_2 nanocrystals could also be one relation. For solar cell performance the (pseudo-) first-order rate constant under steady-state conditions is a relevant parameter as it can give direct information on possible recombination losses due to the reaction of electrons with holes. Analysis of the decay in Figure 6 during the first 1 ms (using a sampling rate of 1 MHz) gives a recombination lifetime of 6 ms . This relatively fast decay proves at least a well pore filling of TiO_2 film by ultra fine particles of pyrite.

4. Conclusion

The pyrite of iron disulfide (FeS_2) shows promise for solar energy conversion devices in photoelectrochemical solar

cells. FeS_2 can be used to sensitize different types of metal oxides. Indirect band gap has been determined for FeS_2 modified MO electrodes. Low performance of the electrodes is mainly due to the presence of multiphase FeS_2 . Looking for a pure and stoichiometric pyrite will be very promising for solar cells based on quantum dots semiconductors.

Acknowledgments

The research project is funded by the National Plan for Science and Technology Program, Grant number 09-NAN859-02, King Saud University, Riyadh, Saudi Arabia. I. Bedja would like to thank Dr. Gerrit Boschloo for his helpful discussions.

References

- [1] B. O'Regan and M. Grätzel, "A low-cost, high-efficiency solar cell based on dye-sensitized colloidal TiO_2 films," *Nature*, vol. 353, no. 6346, pp. 737–740, 1991.
- [2] I. Bedja, S. Hotchandani, and P. V. Kamat, "Preparation and photoelectrochemical characterization of thin SnO_2 nanocrystalline semiconductor films and their sensitization with bis (2,2'-bipyridine)(2,2'-bipyridine-4,4'-dicarboxylic acid)ruthenium(II) complex," *Journal of Physical Chemistry*, vol. 98, no. 15, pp. 4133–4140, 1994.
- [3] I. Bedja, S. Hotchandani, and P. V. Kamat, "Fluorescence and photoelectrochemical behavior of chlorophyll a adsorbed on a nanocrystalline SnO_2 film," *Journal of Applied Physics*, vol. 80, pp. 2180–2187, 1996.
- [4] T. A. Heimer, E. J. Heilweil, C. A. Bignozzi, and G. J. Meyer, "Electron injection, recombination, and halide oxidation dynamics at dye-sensitized metal oxide interfaces," *Journal of Physical Chemistry A*, vol. 104, no. 18, pp. 4256–4262, 2000.
- [5] D. Liu and P. V. Kamat, "Electrochemically active nanocrystalline SnO_2 films: surface modification with thiazine and oxazine dye aggregates," *Journal of the Electrochemical Society*, vol. 142, no. 3, pp. 835–839, 1995.
- [6] R. Vogel, P. Hoyer, and H. Weller, "Quantum-sized PbS , CdS , Ag_2S , Sb_2S_3 , and Bi_2S_3 particles as sensitizers for various nanoporous wide-bandgap semiconductors," *Journal of Physical Chemistry*, vol. 98, no. 12, pp. 3183–3188, 1994.
- [7] J. Rabani, "Sandwich colloids of ZnO and ZnS in aqueous solutions," *Journal of Physical Chemistry*, vol. 93, no. 22, pp. 7707–7713, 1989.
- [8] I. Bedja, S. Holchandani, and P. V. Kamat, "Photosensitization of composite metal oxide semiconductor films," *Berichte der Bunsengesellschaft/Physical Chemistry Chemical Physics*, vol. 101, no. 11, pp. 1651–1653, 1997.
- [9] L. Spanhel and M. J. Anderson, "Semiconductor clusters in the sol-gel process: quantized aggregation, gelation, and crystal growth in concentrated ZnO colloids," *Journal of the American Chemical Society*, vol. 113, no. 8, pp. 2826–2833, 1991.
- [10] G. Boschloo and A. Hagfeldt, "Photoinduced absorption spectroscopy of dye-sensitized nanostructured TiO_2 ," *Chemical Physics Letters*, vol. 370, no. 3–4, pp. 381–386, 2003.
- [11] H. Tributsch, *Structure and Bonding*, vol. 49, p. 128, 1982.
- [12] H. Tributsch, in *Modern Aspects of Electrochemistry*, J. O. Bockris, Ed., vol. 14, chapter 4, Pergamon, Oxford, UK, 1986.
- [13] E. Bucher, "Solar cell materials and their basic parameters," *Applied Physics*, vol. 17, no. 1, pp. 1–26, 1978.
- [14] A. Ennaoui, S. Fiechter, C. Pettenkofer et al., "Iron disulfide for solar energy conversion," *Solar Energy Materials and Solar Cells*, vol. 29, no. 4, pp. 289–370, 1993.
- [15] Y. C. Shen, H. Deng, J. Fang, and Z. Lu, "Co-sensitization of microporous TiO_2 electrodes with dye molecules and quantum-sized semiconductor particles," *Colloids and Surfaces A*, vol. 175, no. 1–2, pp. 135–140, 2000.
- [16] G. Chatzitheodorou, S. Fiechter, M. Kunst, J. Luck, and H. Tributsch, "Low temperature chemical preparation of semiconducting transition metal chalcogenide films for energy conversion and storage, lubrication and surface protection," *Materials Research Bulletin*, vol. 23, no. 9, pp. 1261–1271, 1988.
- [17] C. Bauer, G. Boschloo, E. Mukhtar, and A. Hagfeldt, "Electron injection and recombination in $\text{Ru}(\text{dcbpy})_2(\text{NCS})_2$ sensitized nanostructured ZnO ," *Journal of Physical Chemistry B*, vol. 105, no. 24, pp. 5585–5588, 2001.
- [18] G. Boschloo and A. Hagfeldt, "Photoinduced absorption spectroscopy as a tool in the study of dye-sensitized solar cells," *Inorganica Chimica Acta*, vol. 361, no. 3, pp. 729–734, 2008.
- [19] N. Sakai, Y. Ebina, K. Takada, and T. Sasaki, "Electronic band structure of titania semiconductor nanosheets revealed by electrochemical and photoelectrochemical studies," *Journal of the American Chemical Society*, vol. 126, no. 18, pp. 5851–5858, 2004.
- [20] G. W. Luther, "Pyrite synthesis via polysulfide compounds," *Geochimica et Cosmochimica Acta*, vol. 55, no. 10, pp. 2839–2849, 1991.
- [21] P. Qin, X. Yang, R. Chen et al., "Influence of π -conjugation units in organic dyes for dye-sensitized solar cells," *Journal of Physical Chemistry C*, vol. 111, no. 4, pp. 1853–1860, 2007.
- [22] S. A. Haque, Y. Tachibana, D. R. Klug, and J. R. Durrant, "Charge recombination kinetics in dye-sensitized nanocrystalline titanium dioxide films under externally applied bias," *Journal of Physical Chemistry B*, vol. 102, no. 10, pp. 1745–1749, 1998.

